Linking Seismic and Sub-Seismic Fault Predictions using Laser Scanning of Outcrop Analogues*

By
Richard R. Jones[1], Dave Healy[2], Jonny Imber[2], Ruth Wightman[2], Ken McCaffrey[2], and Bob Holdsworth[2]

Search and Discovery Article #40256 (2007)
Posted September 5, 2007

*Adapted from extended abstract prepared for presentation at AAPG Annual Convention, Long Beach, California, April 1-4, 2007

[1]Geospatial Research Ltd., Durham, UK (richard@geospatial-research.com)
[2]Durham University, UK

Abstract

Although fault models derived from seismic reflection data often provide an excellent view of 3D fault geometries at a large scale, outcrop analogues can give additional geometric and kinematic constraints to help bridge the critical scale-gap needed to integrate seismic and borehole datasets. We use terrestrial laser scanning (ground-based LiDAR) to carry out precise measurements of the 3D geometry of well exposed fracture surfaces. A case study using regular laser-scanning of an active opencast coal mine provides additional constraint, with 3D fault geometries sequentially revealed throughout the rock volume, as the coal face progressively migrates with time.

The laser scan data provide unprecedented detail and allow spatial variation in various fracture attributes to be quantified, including 3D curvature, fracture connectivity, branch-line geometry, relationship between corrugations and fault splays, detailed fault throw profiles, and the spatial correlation between fracture density and fold curvature. Measurement of such fracture parameters, collected from a range of outcrop analogues, provides direct quantitative input for calibration of geomechanical models and for validation of fracture networks derived by deterministic or stochastic methods.

Introduction

Outcrop analogues can give additional geometric and kinematic constraints to help bridge the critical scale-gap needed to integrate seismic and borehole datasets. We use a range of digital survey methods (Figure 1) to capture detailed, spatially referenced outcrop data (Jones et al. 2004; McCaffrey et al. 2005). Of the various methods, Terrestrial Laser Scanning (also commonly called ground-based LiDAR) is usually the most efficient way to capture large amounts of spatially precise data from relevant areas of outcrop. With typical acquisition rates up to 12,000 points a second, laser-scanning makes it possible to rapidly acquire a detailed virtual copy of an outcrop, in which the topography of the outcrop is represented by a point cloud comprising tens or hundreds of millions of points (Figure 2b). With modern high-speed laser scanners (Figs. 1f and 2a), an experienced operator will usually be able to survey many hundred square metres of outcrop per day (depending on the nature of the topography and the level of detail required). In areas of good exposure and 3D topography, laser scanning is therefore an extremely efficient way to study large outcrop analogues of sedimentary and structural architectures on a scale directly comparable to seismically imaged structures, but with 100-1000 times better resolution. In this way, outcrop studies based on laser-scanning can effectively bridge the gap between seismic and borehole datasets.

While laser-scanning has high potential to *enhance* outcrop studies, it is not a replacement for careful geological field work, and in our experience, the most useful approach to studying outcrop analogues is to integrate key geological observations, measurements, and interpretations into the detailed geospatial outcrop model derived from laser-scanning. To facilitate this integration in the field, the precise locations of geological observations and measurements are recorded using either differential Real-Time Kinematic (RTK) GPS (Figure 1a, b) or laser-ranging devices (Figure 1c), or are tied directly to specific points in the laser-scan dataset. RTK GPS is also ideal to enable laser-ranger and laser-scan data to be georeferenced to a global coordinate system.

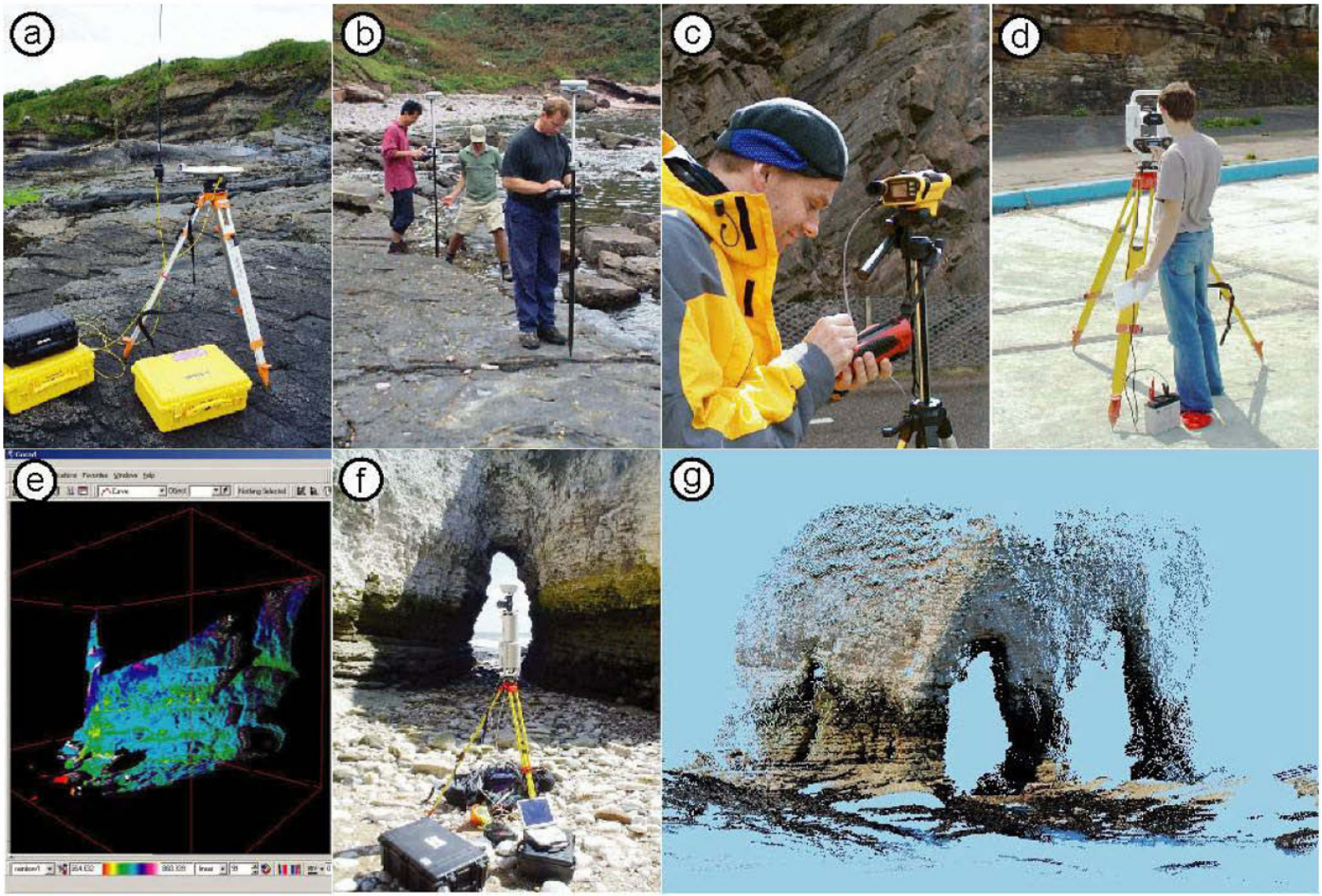

Figure 1. Examples of digital survey methods to capture spatially referenced outcrop data; (a) Real-Time Kinematic (RTK) GPS, stationary base-station. In the field, differential GPS locates the base station with a global accuracy of ca. 0.5m; this is improved by post-processing to ca. 10mm; (b) Two RTK GPS rover-units. A positional fix relative to the base-station can be made instantaneously, typically with a precision of ca. 10mm; (c) MDL LaserAce 300 laser-ranging device, with hand-held PDA data-logger. The laser-ranger is used to record the precise position of individual observations and structural measurements made on the outcrop, relative to the instrument. RTK GPS is then used to measure the accurate location of the instrument, and thus the absolute position of all its relative measurements; (d) terrestrial laser-scanning using MDL Quarryman The data captured includes x,y,z position and intensity information for each point scanned, and the resultant grey-scale laser-scan point-cloud can be imported into most 3D visualisation tools; (e) false-colour laser-scan point-cloud from MDL scanner, imported into GoCad; (f) Riegl LMS-Z360i laser-scanner, with top-mounted high resolution digital camera (to give true-colour point cloud data) and RTK GPS unit to record precise scanner location; (g) true-colour point cloud data from Riegl LMS-Z360i scanner. Locations: (a) analysis of fault-related folding, Howick, NE England (Pearce et al., 2006); (b) segmented faults, Lamberton, SE Scotland; (c) study of onshore analogues for Devonian clastics of West Orkney Basin, Kirtomy, N Scotland; (d-e) faulting in Carboniferous sandstone/shale sequence, NE England; (f-g) study of fractured carbonates, Flamborough, E England.

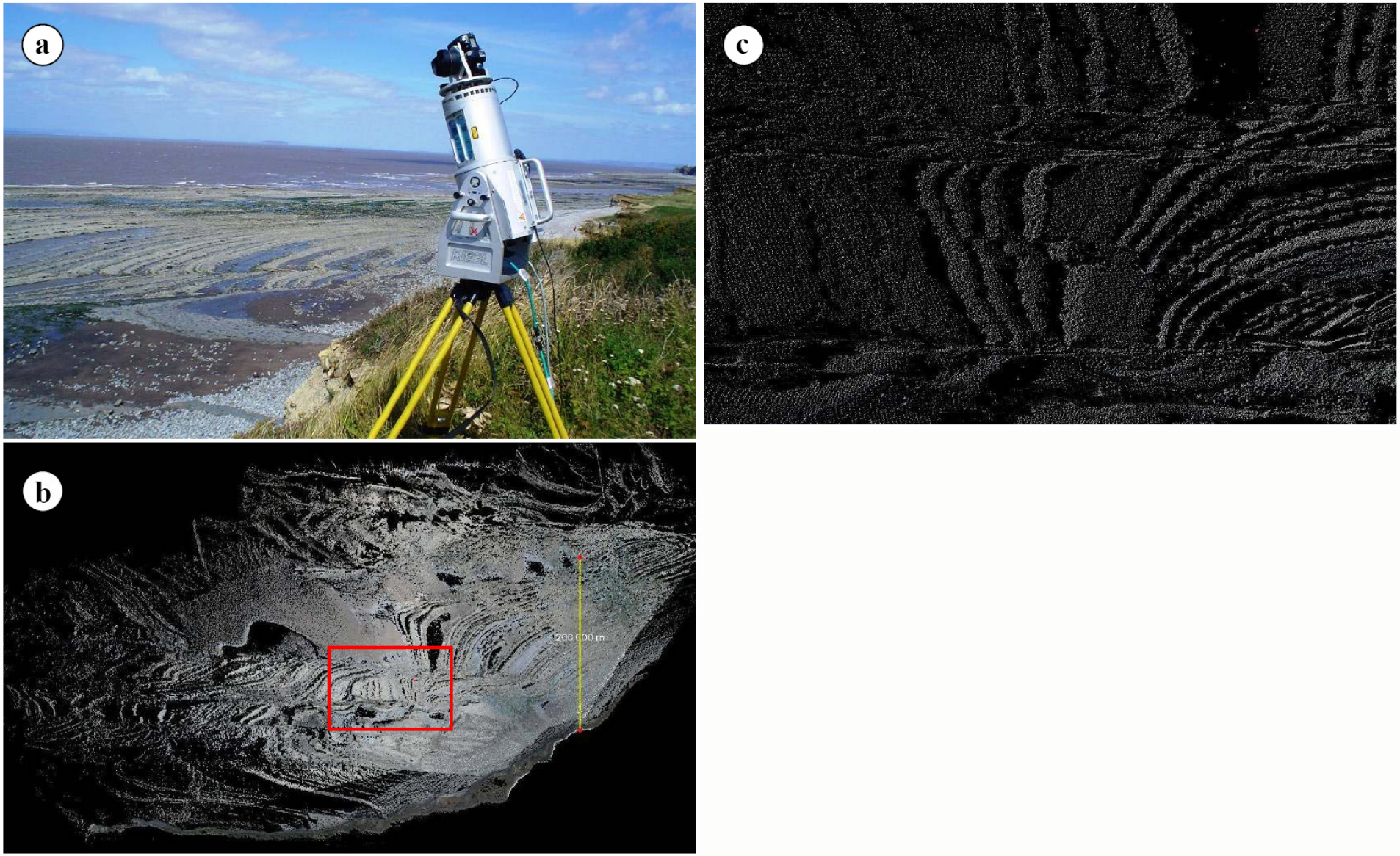

Figure 2. Terrestrial laser-scanning study of fault relay zone architectures in normal faults from Kilve, Somerset, SW England: (a) Riegl LMS Z420i scanner, with tilt-mount to allow the scanner to be pointed downwards to scan the wave-cut platform from the cliff top; (b) Oblique view looking down on part of the laser scan point cloud. Yellow scale bar is 200m; (C) area of detail showing anastomosing fault strands. These can be picked directly within the scan data (comparable to picking faults in seismic), so that fault offsets and displacement gradients can be quantified. The view is approximately 100m wide, and is from the area of the red box in (b).

Outcrop to Basin Scale Models

Additional digital methods are also useful to provide wider geographical and geological context to the virtual outcrop analogue (Figure 3). Integrating the laser-scan data with other more regional datasets, such as aerial images draped over a DEM, subsurface maps, ground-penetrating radar (Pringle et al., 2003), seismic sections and satellite data, make it easier for the geologist to visualise the spatial and scaling relationships between structures seen in outcrop and those of reservoir and basin scale (Jones et al., 2007, *in press*). Equally useful is to isolate the virtual outcrop dataset and to incorporate it directly into a reservoir model from a hydrocarbon field of current interest--to allow the asset team to study the analogue in full detail within the context of their own subsurface volume.

Quantification of Structural Attributes

The laser-scan data provide unprecedented detail and allow spatial variation in various fracture attributes to be quantified, including 3D curvature (Figure 4), fracture connectivity, branch-line geometry, relationship between corrugations and fault splays, detailed fault throw profiles, and the spatial correlation between fracture density and fold curvature. Measurement of such fracture parameters, collected from a range of outcrop analogues, provides direct quantitative input for calibration of geomechanical models and for validation of fracture networks derived by deterministic or stochastic methods. A case study using regular laser-scanning of an active opencast coal mine, provides additional constraint, with 3D fault geometries sequentially revealed throughout the rock volume, as the working coal face progressively migrates with time.

References

Jones, R.R., McCaffrey, K.J.W, Wilson, R.W., and Holdsworth, R.E. 2004. Digital field data acquisition: towards increased quantification of uncertainty during geological mapping, *in* Curtis, A., Wood, R., eds., Geological Prior Information: Geological Society Special Publication 239, p.43-56.

Jones, R.R., McCaffrey, K.J.W., Clegg, P., Wilson, R.W., Holliman, N.S., Holdsworth, R.E., Imber, J., and Waggott, S., 2007 (i*n press*), Integration of regional to outcrop digital data: 3D visualisation of multi-scale geological models: Computers & Geosciences, v.33.

Kokkalas, S., Jones, R.R., McCaffrey, K.J.W., Clegg, P., 2007 (*in press*), Quantitative fault analysis at Arkitsa, Central Greece, using Terrestrial Laser Scanning ("LiDAR"): Bulletin of the Geological Society of Greece, vol. XXXVII, p.2007.

McCaffrey, K.J.W., Jones, R.R., Holdsworth, R.E., Wilson, R.W., Clegg, P., Imber, J., Holliman, N., and Trinks, I. 2005, Unlocking the spatial dimension: digital technologies and the future of geoscience fieldwork: Journal of the Geological Society, London, v. 162, p.927-938.

Pringle, J.K., Clark, J.D., Westerman, A.R., and Gardiner, A.R. 2003, Using GPR to image 3D turbidite channel architecture in the Carboniferous Ross Formation, County Clare, Western Ireland, *in* Bristow, C.S., Jol, H., Eds., GPR in Sediments: Geological Society Special Publication 211, p. 309-320.

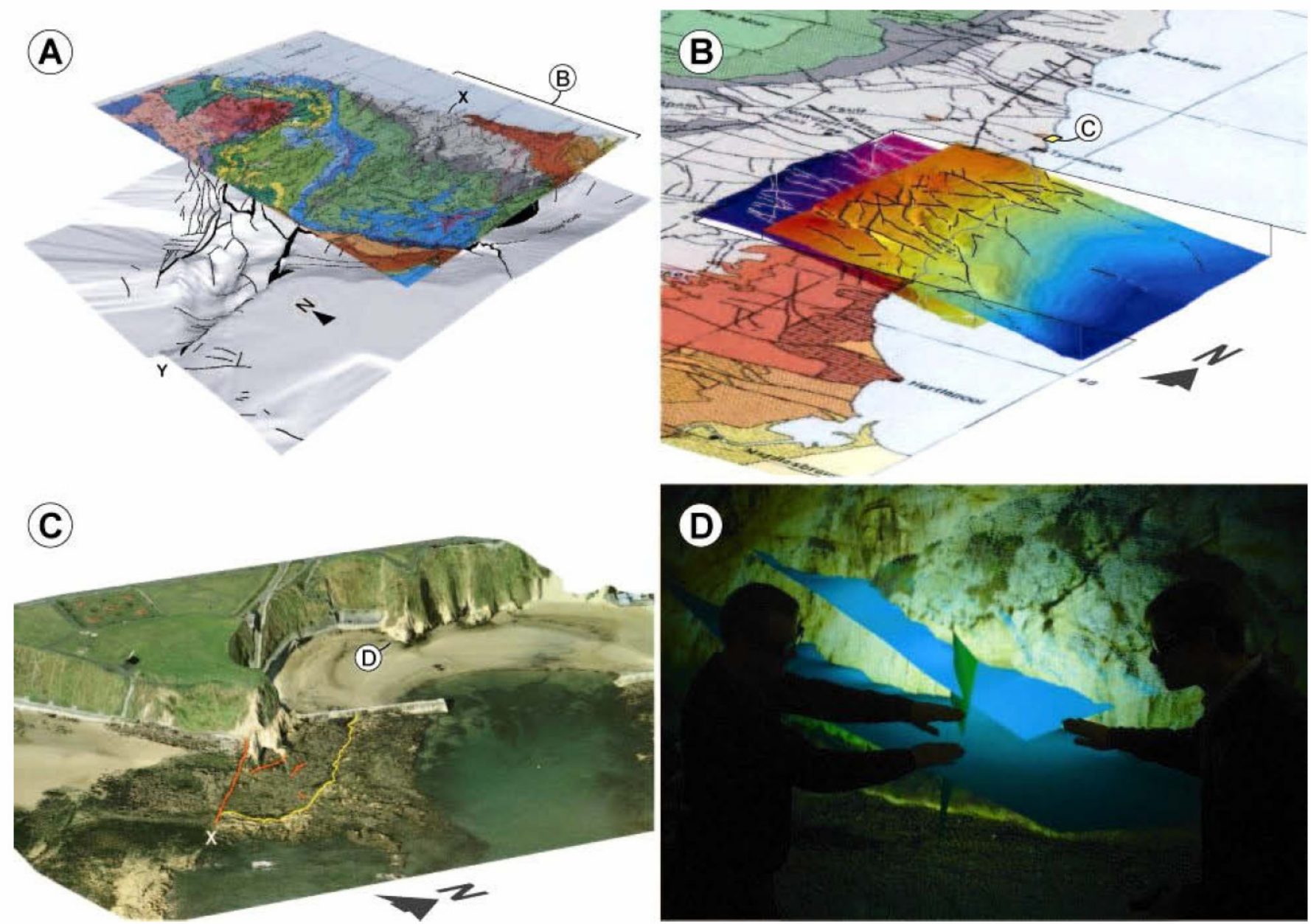

Figure 3. Example of integrated multi-scale 3D geological model from NE England, spanning seven orders of magnitude, from Jones et al. (2007, *in press*): (A) regional scale, showing the solid geology at the Earth's surface, above a surface showing basement topography: field of view ca. 1.6 x 10^5 m. X and Y mark traces of the 90-fathom/Stublick fault system on the surface and at top basement, respectively; (B) subsurface data at sub-regional scale; the Maudlin coal seam (lower surface) and Carboniferous-Permian unconformity (upper surface); width of subsurface area covered ca. 2.5 x 10^4 m. These surfaces are shown embedded within a cut-away geology map of Tyneside-Teesside; (C) local scale with integration of geological boundaries draped onto local topography: X is the trace of 90-fathom fault on the foreshore. The field of view ca. 5 x 10^2 m, location shown in (B); (D) outcrop scale, showing interpretation of detailed terrestrial laser-scan data in an immersive 3D visualisation facility: field of view ca. 3 x 10^1 m, location given in (C); laser-scan point spacing ca. 2 x 10^{-2} m.

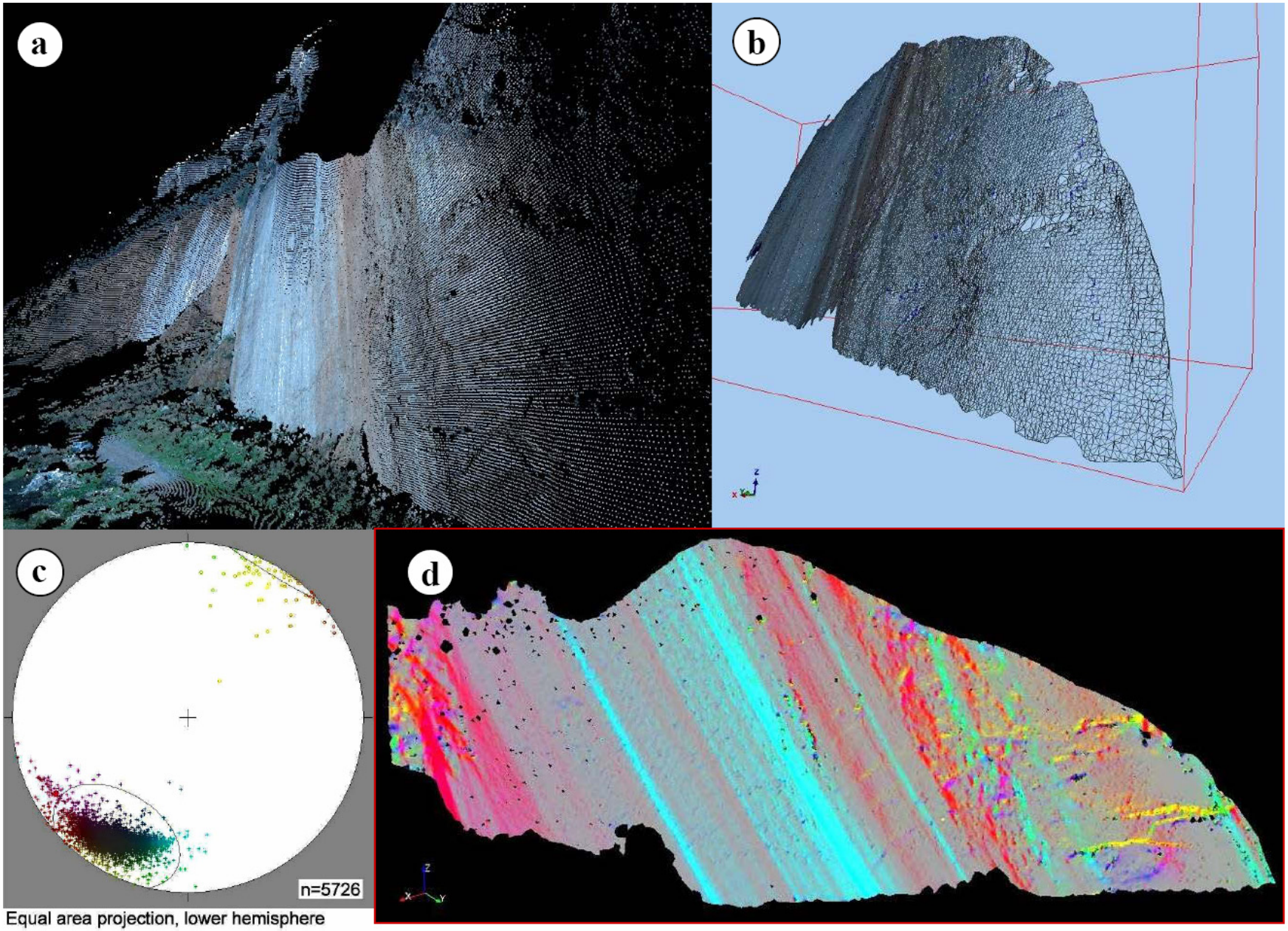

Figure 4. Laser scan from spectacularly exposed neotectonic faults at Arkitsa, Gulf of Evia, Greece (Kokkalas et al., 2007, *in press*): (a) Laser scan point cloud. Polished areas of fault surface in foreground and background are two separate fault panels; (b) filtered and meshed surface from the fault panel shown in the foreground of (a), consisting of ca. 117,000 polygons, derived from 10 million laser scan points. Fault panel is 65m high; (c) Stereonet showing the orientation of a subset (N=5726) of the normals (i.e., poles) to polygons from the mesh shown in (b). Colours correspond to orientation of each normal relative to the mean orientation. (d) colours from (c) re-projected onto the meshed fault surface, to emphasise changes in orientation of the surface. This makes it easier to visualise fault curvature, corrugations, and small-scale rupturing and fracturing of the fault surface.